1995

NASA/ASEE SUMMER FACULTY FELLOWSHIP PROGRAM

MARSHALL SPACE FLIGHT CENTER
THE UNIVERSITY OF ALABAMA IN HUNTSVILLE

IMPELLER LEAKAGE FLOW MODELING FOR MECHANICAL VIBRATION CONTROL

Prepared By:	Alan B. Palazzolo, Ph.D
Academic Rank:	Associate Professor
Institution and Department:	Texas A&M University Mechanical Engineering
NASA/MSFC:	
Office:	Structures & Dynamics Laboratory
Division:	Control System
Branch:	Mechanical Systems Control
MSFC Colleague(s):	Steve Ryan, Ph.D

INTRODUCTION

HPOTP and HPFTP vibration test results have exhibited transient and steady characteristics which may be due to impeller leakage path (ILP) related forces. For example, an axial shift in the rotor could suddenly change the ILP clearances and lengths yielding dynamic coefficient and subsequent vibration changes. ILP models are more complicated than conventional-single component-annular seal models due to their radial flow component (coriolis and centrifugal acceleration), complex geometry (axial/radial clearance coupling), internal boundary (transition) flow conditions between mechanical components along the ILP and longer length, requiring moment as well as force coefficients. Flow coupling between mechanical components results from mass and energy conservation applied at their interfaces. Typical components along the ILP include an inlet seal, curved shroud, and an exit seal, which may be a stepped labyrinth type. Von Pragenau (MSFC) has modeled labyrinth seals as a series of plain annular seals for leakage and dynamic coefficient prediction. These multi-tooth components increase the total number of "flow coupled" components in the ILP.

Childs' (1987) developed an analysis for an ILP consisting of a single, constant clearance shroud with an exit seal represented by a lumped flow-loss coefficient. This same geometry was extended to include compressible flow by Nhai The Cao and Childs (1993). The latter reference did not discuss dynamic coefficients, presumably due to their highly non-quadratic results for impedance vs whirl frequency. These "resonances" appear in both references and are reported to be caused by the centrifugal acceleration term of the path momentum equations. Test impedances measured by Guizburg (1995) at Cal Tech (1992) do not contain the resonances and appear quite apt to be accurately described by quadratic functions of whirl frequency.

The objective of the current work is to:

(a) Supply ILP leakage-force-impedance-dynamic coefficient modeling software to MSFC engineers. The initial model will be based on incompressible/compressible bulk flow theory.

(b) Design the software to model a generic geometry ILP described by a series of components lying along an arbitrarily directed path.

(c) Validate the software by comparison to available test data, CFD and bulk models.

(d) Develop a hybrid CFD-bulk flow model of an ILP to improve modeling accuracy within practical run time constraints.

RESULTS

A. Theory

The governing equations consisted of continuity (mass conservation), momentum and equation of state (thermophysical properties). The momentum equations were obtained from the cylindrical coordinate Navier-Stokes equations by imposing:

(a) The kinematic constraint of uniform (rectangular) velocity profiles through the film thickness.

(b) Zero pressure gradient through the film thickness.

(c) Velocity components perpendicular to flow path are zero.

(d) The perpendicular to the flow path intersects stator and rotor at equal distances ($\pm$ H/2).

Time and circumferential derivatives are set to zero to obtain the steady state (zeroeth order) differential equation. The primitive constitutive and clearance variables (u, w_s, p, q, m, h) are expressed as sums of their steady state values plus their perturbation values. The latter resulting from infinitesimally small, circular, cylindrical and conical whirl orbits. Cancellation of second order terms provides the governing P.D.E.'s for the perturbation variables (u_1, w_s, p_1, q_1, and m_1). The P.D.E.'s are transformed to O.D.E.'s by separating out their harmonic time and circumferential dependencies. Both zeroeth and first order problems are solved as nonlinear and linear, two point boundary value problems, respectively. Runge Kutta 4th order numerical integration is employed in both problems. Internal transition conditions of mass, energy and angular momentum conservation are imposed at the interfaces between individual components in the ILP.

Forces and moments perturbation eccentricity and angle, i.e. impedances, are determined by integrating first order pressure and shear stresses along the rotor length. Quadratic curve fits of the impedances vs whirl frequency ration yield a set of 24 independent stiffness, damping, and inertia coefficients. These dynamic coefficients or impedance functions may then be used as input to turbopump rotordynamic codes for mechanical system vibration control.

B. Examples

Various shock cases were formulated to help validate the ILP modeling software. These

(b) Published data for dynamic coefficients of a linear-clearance tapered seal of length L. The ILP was modeled as a "constant radius" shroud of length 3 L/4 and an exit seal of length L/4. The radius and linear taper profile of the original seal was maintained in the ILP model.

(c) Published results of Childs' (1987) simulation of an ILP including a linear-radius profile shroud and plain annular exit seal.

The results for check case (a) show near perfect agreement as seen in Table 1. The results of check case (b) again showed near perfect agreement for leakage rate and all dynamic coefficients. The check case (c) geometry is shown in Figure 1 with parameters given in Table 2. The predicted leakage rates vs exit seal clearances showed excellent agreement with Childs' as shown in Table 3. Figure 2 shows a comparison of predicted impedances with Childs' results. Although agreement is very good for the radial impedance the tangential impedances are significantly different. The dynamic coefficients contributed by the shroud and by the seal in the ILP show fair agreement with Childs' as shown in Table 4. Discrepancies in the results may have resulted in different input data since the following parameters were not specified in Childs' model;

*Seal Hir's constants

* Seal inlet loss factor (assumed to be same as shroud inlet loss factor (0.1).

* Frequency ratios used in impedance curse fit (0.5, 1.25. 2.0, used in current analysis).

* Shroud clearance profile used by Childs (assumed to be constant at 5.8 mm).

The total coefficients for the ILP are obtained as the sums of the shroud and seal contributions in Table 4.

CONCLUSIONS

A bulk flow based computer model has been developed for obtaining ILP dynamic forces due to cylindrical and conical perturbation orbits of the shaft. These forces vary with whirl orbit frequency and are curve fit to obtain stiffness, mass, and damping coefficients. Future plans

Table 1. **Closed form solution for frictionless flow through Shroud and Exit Wear-ring Seal**

Particulars	*Closed Form Solution*	*Current Analysis*
Shroud Inlet Path Velocity, Ws(0) (m/s)	0.918	0.9193
Shroud Exit Path Velocity, Ws(L) (m/s)	1.361	1.3626
Shroud Inlet Pressure, P(0) (N/m2)	465,536.5	465,640.6
Shroud Exit Pressure, P (N/m2)	26,363.2	26,420.56
Shroud Exit Swirl Velocity, U(L) (m/s)	27.16	27.163
Leakage, Q (kg/s)	5.85	5.859

Table 2. **Bolleter et al. Shrouded Impeller Test Results and comparison with Childs (1989)**

Input Data :

$\Delta P = 0.466 MPa$	*Working Fluid: Water*	$\rho = 1000 kg/m^3$	$\mu = 1.3E\text{-}03\ Pa\text{-}s$
Shrd. InletLoss, $\xi = 0.1$ *SealInletLoss*, $\xi = 0.1$	*Shroud*: $C_i = C_0 = 5.8mm$ *Seal*: $C_i = C_0 = 0.36\ mm$	*Speed*, $N = 2000 rpm$	*Shrd. Length*$L_s = 64mm$ $dr/ds = -0.89$ *SealLength*$l_{si} = 33mm$
Shrd. Inl. Dia = 175 *mm* *SealInl. Dia* = 118 *mm*	*Preswirl*, $\gamma = 0.5$	*Shroud* $n_s, m_s = 0.079, -0.25$ *Seal* $n_s, m_s = 0.079, -0.25$	*Shroud* $n_s, m_s = 0.079, -0.25$ *Seal* $n_s, m_s = 0.079, -0.25$

Table 3. *Comparison of* ***Leakage (kg/s)*** *with Childs (1989) for various Wear-ring seal clearances*

Wear-ring seal Clearance (in mm)	*Childs*	*Current Analysis*
0.36	4.03	3.886
0.54	6.241	6.425
0.72	8.432	8.594

Table 4 ILP Dynamic Coefficients

	Shroud		Seal	
Coefficient	Current	Childs	Current	Childs
K	64,472. n/m	60,050 n/m	1,870,000 n/m	612,000.
k	196,724. n/m	199,700 n/m	1,340,000 n/m	463,000.
C	951. N.s./m	1,200. N.s./m	7329. N.s/m.	3356.
c	105. N.s./m	682 N.s./m	440. N.s./m.	79.
M	1.09 Kg.	2.51 Kg.	3.08 Kg.	.311
m	-.715 Kg.	0.01 Kg.	-1.3 Kg.	.08

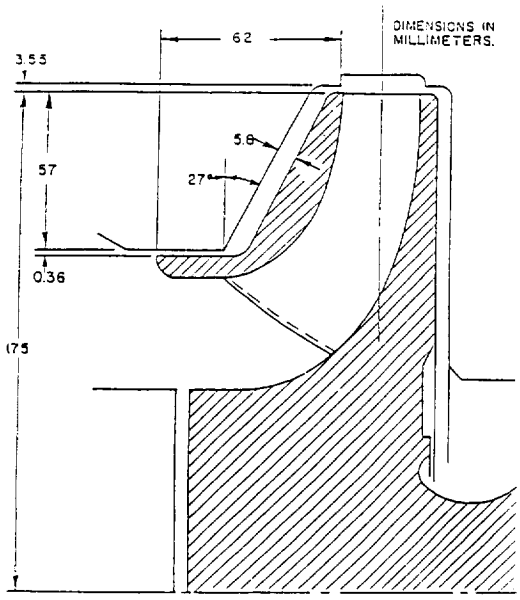

Figure 1. Example impeller; Bolleter

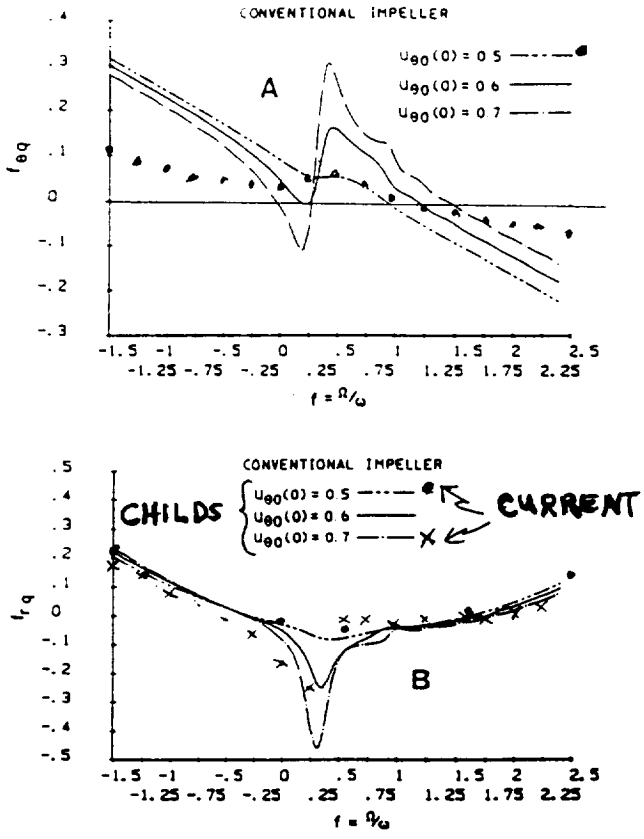

Figure 2. Nomdimensional force coefficients for the conventional impeller (a) tangential-force coefficient, (b) radial-force coefficient